

Size Fractionation of Metal Nanoparticles by Membrane Filtration**

By Ariya Akthakul, Allon I. Hochbaum, Francesco Stellacci, and Anne M. Mayes*

Metal^[1,2] and semiconductor^[3–5] nanoparticles displaying unique optical^[6] and electronic^[7] properties beyond their bulk analogues are widely being developed for applications in sensors,^[8] diagnostics, and biological labeling.^[9,10] The optoelectronic properties of these materials depend strongly on particle size and uniformity.^[11–14] Nanoparticle syntheses involve nucleation and growth mechanisms that are fluctuation driven in nature, giving rise to a finite size distribution of product particles.^[15–17] For micrometer-sized colloidal metal particles, a narrow size distribution can be simply achieved post-synthesis using commercial techniques such as ultracentrifugation or microfiltration.^[18] However, for nanometer-sized particles, the length scale of fluctuations becomes comparable to the average particle size. Separation methods have been limited to date to low-volume, time-intensive techniques such as size-exclusion chromatography,^[19,20] fractional crystallization,^[21] and gel electrophoresis.^[22] A membrane-based filtration process for nanoparticle fractionation could greatly facilitate their commercialization by providing high-speed, high-volume fractionation capability.^[23–25] However, membranes prepared by the conventional immersion precipitation process typically display sparse porosity with a broad pore size distribution,^[26] limiting their utility for such applications.

In this work, we introduce a novel thin film composite nanofiltration (NF) membrane incorporating a self-assembling graft copolymer with a hydrophobic poly(vinylidene fluoride) (PVDF) backbone and hydrophilic poly(oxyethylene methacrylate) (POEM) side chains.^[27] Phase separation of the backbone and side chains results in the creation of a bicontinuous structure with uniformly sized nanoscale channels of poly(ethylene oxide) (PEO) for size-controlled transport surrounded by a semicrystalline PVDF hydrophobic matrix for structural support.^[27] (The bicontinuous morphology is described in separate publications).^[27–29] Using such membranes, we demonstrate the fractionation of monolayer-protected gold nanoparticles to achieve a well-defined cutoff diameter

and reduced size dispersity. The ability to tune the separation characteristics of the NF membranes is demonstrated through the use of nanoparticle ligand exchange, choice of solvent, and particle transport kinetics.

A self-assembling PVDF-*g*-POEM graft copolymer with 39.5 wt.-% POEM and ~23 ethylene oxide (EO) repeat units per side chain was synthesized by atom transfer radical polymerization using PVDF (number-average molecular weight ~107 000 g mol⁻¹) as a macroinitiator, following methods previously published.^[27,28] A series of composite NF membranes was prepared, each membrane consisting of a ~0.5 μm non-porous layer of PVDF-*g*-POEM coated onto a commercial PVDF ultrafiltration membrane (Pall Corp.).

Gold nanoparticles were synthesized via a modification of the Schriffin method^[30] using a 1:3 octanethiol (HS-C₈) ligand to gold molar ratio. In toluene solution, their size dispersity is detected in the UV-vis spectrum as a broadening of the gold surface plasmon resonance peak at ~520 nm superimposed on the absorption baseline due to Rayleigh scattering, as seen in Figure 1a.^[31,32] Direct counting of nanoparticle diameters from several transmission electron microscopy (TEM) images such as that in Figure 1b reveals sizes ranging from ~1–6 nm.

Filtration of the nanoparticle solution through the NF membrane allows smaller nanoparticles to permeate. The UV-vis

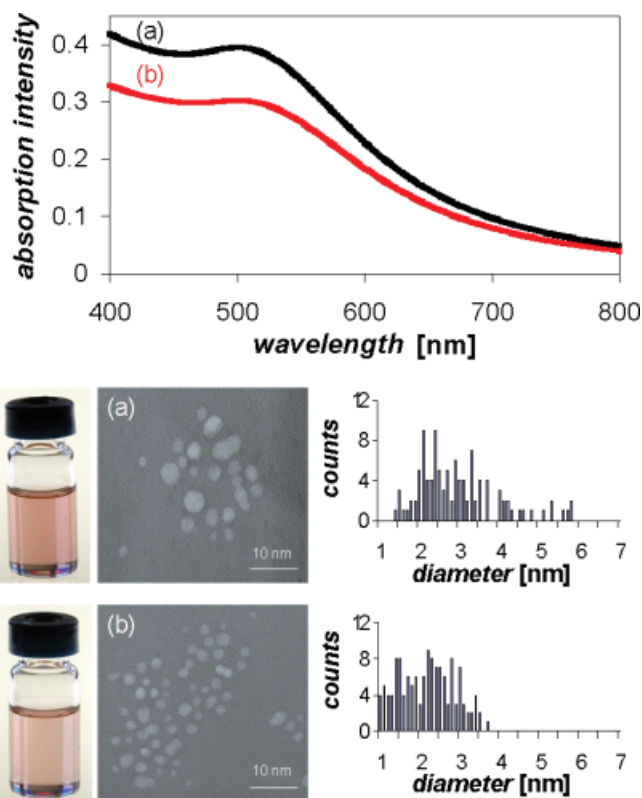


Figure 1. Optical absorption spectra and TEM images with metal core size statistics of nanoparticles prepared with 1:3 molar ratio of HS-C₈/Au in toluene. a) Feed solution (average size ~3.0 ± 1.0 nm); b) solution permeated through PVDF-*g*-POEM-coated membrane with cutoff ~3.8 nm (average size ~2.2 ± 0.7 nm).

[*] Prof. A. M. Mayes, Dr. A. Akthakul, A. I. Hochbaum, Prof. F. Stellacci
Department of Materials Science and Engineering
Massachusetts Institute of Technology
Cambridge, MA 02139 (USA)
E-mail: amayes@mit.edu

[**] The authors acknowledge Michael Frongillo at Massachusetts Institute of Technology (MIT) for his assistance with TEM. Financial support for this work is provided by the Office of Naval Research under grant no. N00014-02-1-0343 and by the National Science Foundation NIRT program grant no. DMR-0303973, and in part by the NSF MRSEC program under award no. DMR-0213282.

spectrum of the permeate solution exhibits a decrease in the slope of the absorption baseline, indicating a smaller average particle size, while TEM images reveal that nanoparticles with a metal core diameter larger than 3.8 nm are excluded from the channels, as shown in Figure 1b. Filtration thus resulted in a decrease of the average nanoparticle diameter and standard deviation from 3.0 ± 1.0 nm to 2.2 ± 0.7 nm. The cutoff diameter is consistent with the expected dimensions of the solvent-filled POEM nanochannels.^[27–29]

Because the metal core and the protective ligand shell jointly govern the effective size of these gold nanoparticles, an increase in the shell size through use of a longer ligand should decrease the largest permeable metal core diameter, under the same filtration environment. Here, we increased the ligand length from 8 to 18 hydrocarbon units through synthesis using a 1:1 octadecanethiol (HS-C₁₈) to gold molar ratio and filtered the solution in toluene through the PVDF-g-POEM coated membrane. As anticipated, the metal core size cutoff in the permeate solution was reduced because of the larger ligand shell, as seen in Figure 2. The cutoff diameter of 3.2 nm suggests that the C₁₈ chains do not exhibit all *trans* configurations in solution, as opposed to their behavior in solid state.^[1] This may be due to the fact that, in solution, the ligands are in a dynamic equilibrium between an adsorbed form on the metal core

and a free fully solvated form. Nonetheless, this experiment demonstrates the tunability in the metal core size cutoff using different lengths of the particles' ligands, which can be easily placed on the nanoparticle surface either during the synthesis^[1,30] or via subsequent ligand place exchange reactions.^[1,33,34]

An alternate means of tuning the permeate particle distribution exploits changes in the effective particle diameter and nanochannel width in different solvent media. For this experiment, a ligand exchange reaction was performed to substitute a 3-mercaptopropionic acid (HS-C₂COOH) ligand onto nanoparticle products obtained from a 3:1 HS-C₈ to gold reaction ratio. The reaction was performed so as to yield nanoparticles with a 2:1 octanethiol/mercaptopropionic acid mixture in the ligand shell.^[33,35] The carboxylic acid group renders the resulting nanoparticles soluble not only in toluene, but also in ethanol and water. Filtration of these nanoparticles through the composite NF membrane results in greater exclusion effects with increasing H-bonding capability of the solvent, as evidenced by the UV-vis spectra (not shown) and counting statistics gathered from TEM images (Fig. 3). For a feed solution with particle sizes up to 5.5 nm and average particle size of 3.1 ± 1.0 nm, the cutoff diameter and average

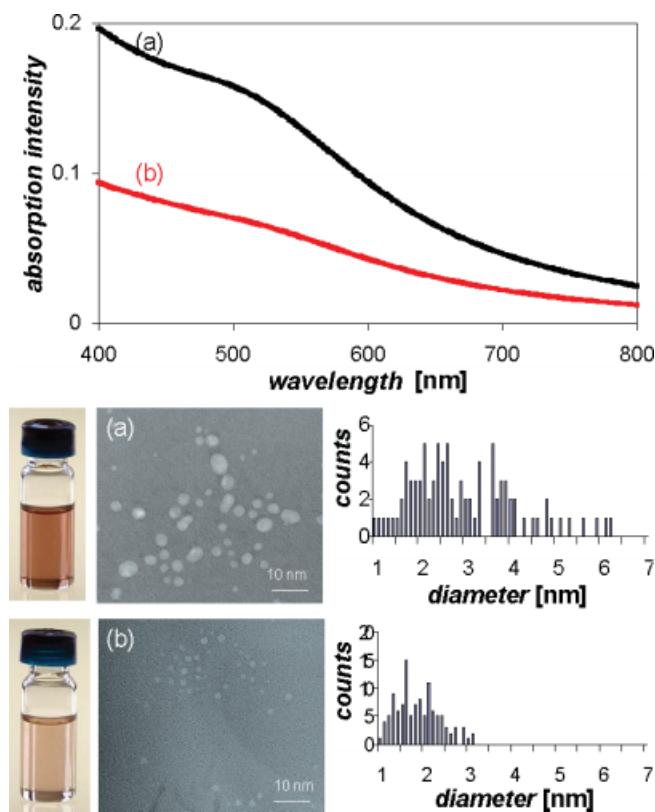


Figure 2. Optical absorption spectra and TEM images with metal core size statistics of nanoparticles prepared with 1:1 molar ratio of HS-C₁₈/Au in toluene. a) Feed solution (average size $\sim 3.0 \pm 1.2$ nm); b) solution permeated through PVDF-g-POEM-coated membrane with cutoff ~ 3.2 nm (average size $\sim 1.9 \pm 0.5$ nm).

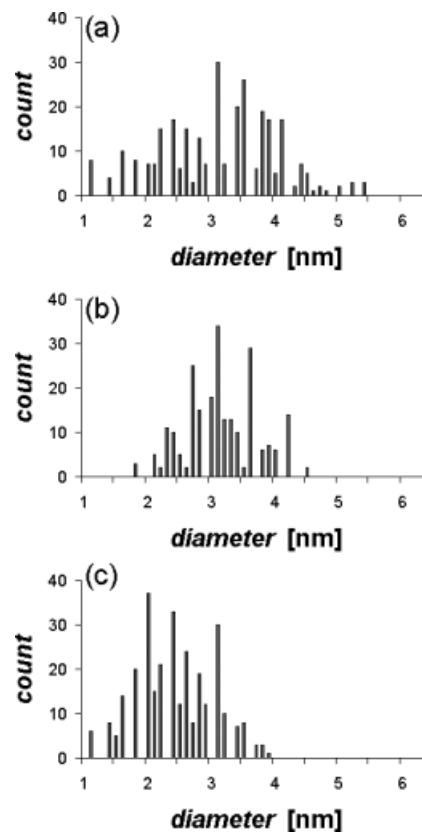


Figure 3. Metal core size statistics from TEM images of nanoparticles prepared with 3:1 molar ratio of HS-C₈/Au and substituted with 3-mercaptopropionic acid ligand. In comparison to a) the feed solution with size up to ~ 5.5 nm (average size $\sim 3.1 \pm 1.0$ nm), samples were collected from the permeate through PVDF-g-POEM-coated membrane in toluene (b) with the cutoff ~ 4.3 nm (average size $\sim 3.0 \pm 0.6$ nm); and in ethanol (c) with the cutoff ~ 4.0 nm (average size $\sim 2.4 \pm 0.6$ nm).

particle size of the permeate were found to be 4.3 nm and 3.0 ± 0.6 nm, respectively, in toluene, and 4.0 nm and 2.4 ± 0.6 nm, respectively, in ethanol. Filtration in water yielded no discernable nanoparticles in the permeate solution.

Solvent polarity affects the swelling of PEO chains lining the nanochannels. In water, the PEO chains are expected to swell substantially, creating a steric barrier to nanoparticle transport. By utilizing binary solvent mixtures, the degree of swelling of the PEO “brush” layer might thus be tuned^[36,37] to achieve a specified cutoff diameter, allowing fractionation of nanoparticles to a high degree of precision.

Finally, the size-dependent diffusivity of the particles was exploited to demonstrate size chromatographic fractionation using the nanofiltration membranes. Figure 4 shows the UV-vis spectra from the permeate solution as a function of time for filtration of nanoparticles synthesized with 1:1 HS-C₁₈ to gold molar ratio in toluene through the PVDF-*g*-POEM-coated membrane. The observed increase in slope of the Rayleigh scattering with time indicates the increase in average particle size as larger particles manage to permeate through the membrane. TEM images of the permeate at these times confirm an increase in average particle size over time from 2.1 ± 0.4 nm at 82 min to 2.4 ± 0.4 nm at 493 min, where the feed solution contained particles as large as 5.6 nm with an average diameter 3.3 ± 1.0 nm. The design of membranes with a thicker selective layer to create a longer diffusion pathway should yield elution times sufficiently long to separate permeate species of defined size, analogous to the approach of Wilcoxon et al.,^[20,38,39] but with the cost and volume advantages of a membrane filtration process.

In conclusion, conventional PVDF ultrafiltration membranes coated with a self-assembling amphiphilic graft copolymer were used to fractionate monolayer-protected Au nanoparticles in a rapid and convenient manner relative to current available techniques.

As the largest size of the filtered particles is limited by the channel width and effective nanoparticle diameter, a series of filtration steps through membranes of different channel widths (by synthesis or solvent choice) or coupled with ligand exchange reactions (to modify the effective diameter) should allow isolation of nanoparticles of a specific size distribution. One-step fractionation might also be possible employing the composite NF membranes as size-chromatographic devices. Other parameters that might be exploited to enhance fractionation capability which remain to be explored include temperature, pressure, and applied electric field.

A complementary finding of these studies is the ability to identify the dynamic sieving characteristics of nanofiltration membranes using nanoparticle probes. Because the channel width is influenced by its swelling behavior in solution, the dynamic width can be indirectly measured via the largest filtered particles. Such understanding of membrane exclusion mechanisms can feed back into membrane design to improve selectivity and flux performance.

Experimental

Synthesis of Monolayer-Protected Gold Nanoparticles: Hydrogen tetrachloroaurate trihydrate, tetraoctylammonium bromide, sodium borohydride, and the ligands octanethiol (HS-C₈), octadecanethiol (HS-C₁₈), and 3-mercaptopropionic acid (HS-C₂COOH) were purchased from Aldrich and used as received. Monolayer-protected gold nanoparticles of varying size and functionality were prepared using a modification of the Schrifin method [30]. The general procedure was to dissolve 354 mg (0.9 mmol) of HAuCl₄·3H₂O in 50 mL of water and 2.187 g (4 mmol) of BrN((CH₂)₇CH₃)₄ in 80 mL of toluene. The two phases were mixed and left stirring for 30 min. Alkane thiol ligand was subsequently introduced into to the reactor, and the solution was allowed to react for 10 min, acquiring a typical white color. A 10 mM solution (30 mL) of NaBH₄ was then added dropwise over a 1 h period, and the solution left stirring for an additional 2 h. The phases were separated and the organic phase was collected, reduced to 10 mL, diluted with 100 ml of absolute ethanol, and placed in a refrigerator overnight. The precipitate was collected via vacuum filtration using quantitative paper filters and extensively washed with water, acetone, and ethanol. Typically, the collected black powder weighed ~100 mg. Place exchange reactions were performed following published methods [33].

Filtration: Reagent grade toluene, acetone, and ethanol were purchased from VWR. Deionized water (dW) of 18 MΩ cm resistivity was prepared using a Millipore (Bedford, MA) Milli-Q filtration system. The filtration experiments were performed i) on 49 mm diameter composite membranes using a Sepa stirred, dead-end filtration

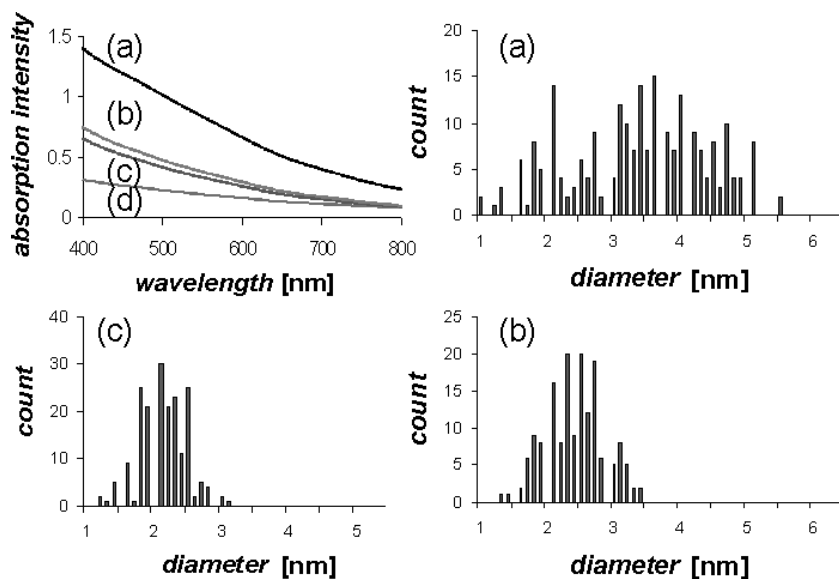


Figure 4. Optical absorption spectra and metal core size statistics from TEM images of nanoparticles prepared with 1:1 molar ratio of HS-C₁₈/Au in toluene. In comparison to a) the feed solution with size up to ~5.6 nm (average size ~ 3.3 ± 1.0 nm), samples were collected from the permeate through PVDF-*g*-POEM-coated membrane at incremental times: d) 38 min; c) 82 min with the cutoff ~3.2 nm (average size ~ 2.1 ± 0.4 nm); b) 493 min with the cutoff ~3.5 nm (average size ~ 2.4 ± 0.4 nm). Due to low particle concentration, no TEM images at 38 min were collected.

cell (Osmonics) with an effective filtration area of 16.9 cm² or ii) on 43 mm diameter membranes using an Amicon 8050 stirred, dead-end filtration cell (Millipore) having an effective filtration area of 13.4 cm². Each filtration cell was stirred at 500 rpm using a speed-adjustable stir plate (VWR) to prevent concentration polarization at the sample surface. Trans-membrane pressure gradients were provided with nitrogen gas during the filtration experiments. Filtration experiments were conducted at 66 psi.

Characterization of Gold Nanoparticles: Nanoparticle diameters in the feed and permeate solutions were determined by transmission electron microscopy (TEM) using a JEOL 100CX microscope operating in bright field mode at 200 kV. TEM specimens for each sample were prepared by evaporating the nanoparticle solution at room temperature onto a 400-mesh copper TEM grid (Ted Pella, Inc.). Image analysis and particle counting were performed using NIH Scion Image software. In the TEM images, apparent agglomerated particles with dimensions over an order of magnitude larger than the average size were neglected. The size distribution of the gold nanoparticles was investigated by UV-vis spectroscopy using a Cary 5E spectrophotometer (Varian).

Received: April 27, 2004
Final version: August 3, 2004

- [1] A. C. Templeton, M. P. Wulfing, R. W. Murray, *Acc. Chem. Res.* **2000**, *33*, 27.
- [2] M.-C. Daniel, D. Astruc, *Chem. Rev.* **2004**, *104*, 293.
- [3] A. P. Alivisatos, P. F. Barbara, A. W. Castleman, J. Chang, D. A. Dixon, M. L. Klein, G. L. McLendon, J. S. Miller, M. A. Ratner, P. J. Rossky, S. I. Stupp, M. E. Thompson, *Adv. Mater.* **1998**, *10*, 1297.
- [4] S. A. Empedocles, M. G. Bawendi, *Science* **1997**, *278*, 2114.
- [5] A. P. Alivisatos, *Science* **1996**, *271*, 933.
- [6] S. A. Empedocles, R. Neuhauser, K. Shimizu, M. G. Bawendi, *Adv. Mater.* **1999**, *11*, 1243.
- [7] R. P. Andres, T. Bein, M. Dorogi, S. Feng, J. I. Henderson, C. P. Kubiak, W. Mahoney, R. G. Osifchin, R. Reifenberger, *Science* **1996**, *272*, 1323.
- [8] A. N. Shipway, E. Katz, I. Willner, *ChemPhysChem* **2000**, *1*, 18.
- [9] A. N. Shipway, M. Lahav, I. Willner, *Adv. Mater.* **2000**, *12*, 993.
- [10] M. Bruchez, M. Moronne, P. Gin, S. Weiss, A. P. Alivisatos, *Science* **1998**, *281*, 2013.
- [11] M. A. Hines, G. D. Scholes, *Adv. Mater.* **2003**, *15*, 1844.
- [12] M. G. Bawendi, M. L. Steigerwald, L. E. Brus, *Annu. Rev. Phys. Chem.* **1990**, *41*, 477.
- [13] S. W. Chen, R. S. Ingram, M. J. Hostetler, J. J. Pietron, R. W. Murray, T. G. Schaaff, J. T. Khoury, M. M. Alvarez, R. L. Whetten, *Science* **1998**, *280*, 2098.
- [14] S. W. Chen, R. W. Murray, S. W. Feldberg, *J. Phys. Chem. B* **1998**, *102*, 9898.
- [15] B. K. H. Yen, N. E. Stott, K. F. Jensen, M. G. Bawendi, *Adv. Mater.* **2003**, *15*, 1858.
- [16] H. Zhang, Z. C. Cui, Y. Wang, K. Zhang, X. L. Ji, C. L. Lu, B. Yang, M. Y. Gao, *Adv. Mater.* **2003**, *15*, 777.
- [17] M. J. Hostetler, A. C. Templeton, R. W. Murray, *Langmuir* **1999**, *15*, 3782.
- [18] H. P. Zheng, I. Lee, M. F. Rubner, P. T. Hammond, *Adv. Mater.* **2002**, *14*, 569.
- [19] V. L. Jimenez, M. C. Leopold, C. Mazzitelli, J. W. Jorgenson, R. W. Murray, *Anal. Chem.* **2003**, *75*, 199.
- [20] J. P. Wilcoxon, J. E. Martin, P. Provencio, *Langmuir* **2000**, *16*, 9912.
- [21] T. G. Schaaff, M. N. Shafiqullin, J. T. Khoury, I. Vezmar, R. L. Whetten, W. G. Cullen, P. N. First, C. Gutierrez-Wing, J. Ascensio, M. J. Jose-Yacaman, *J. Phys. Chem. B* **1997**, *101*, 7885.
- [22] T. G. Schaaff, G. Knight, M. N. Shafiqullin, R. F. Borkman, R. L. Whetten, *J. Phys. Chem. B* **1998**, *102*, 10643.
- [23] M. E. Davis, *Nature* **2002**, *417*, 813.
- [24] W. H. Baur, *Nat. Mater.* **2003**, *2*, 17.
- [25] P. K. Kang, D. O. Shah, *Langmuir* **1997**, *13*, 1820.
- [26] A. Akthakul, W. F. McDonald, A. M. Mayes, *J. Membr. Sci.* **2002**, *208*, 147.
- [27] J. F. Hester, P. Banerjee, Y. Y. Won, A. Akthakul, M. H. Acar, A. M. Mayes, *Macromolecules* **2002**, *35*, 7652.
- [28] S. Inceoglu, S. C. Olugebefola, M. H. Acar, A. M. Mayes, *Des. Monomers Polym.* **2004**, *7*, 181.
- [29] A. Akthakul, R. F. Salinaro, A. M. Mayes, *Macromolecules* **2004**, *37*, 7663.
- [30] M. Brust, M. Walker, D. Bethell, D. J. Schiffrin, R. Whyman, *J. Chem. Soc., Chem. Commun.* **1994**, 801.
- [31] U. Kreibitz, M. Vollmer, *Optical Properties of Metal Clusters*, Springer-Verlag, New York **1995**, p. 25.
- [32] S. Link, M. A. El-Sayed, *Int. Rev. Phys. Chem.* **2000**, *19*, 409.
- [33] R. S. Ingram, M. J. Hostetler, R. W. Murray, *J. Am. Chem. Soc.* **1997**, *119*, 9175.
- [34] W. P. Wulfing, F. P. Zamborini, A. C. Templeton, X. G. Wen, H. Yoon, R. W. Murray, *Chem. Mater.* **2001**, *13*, 87.
- [35] A. M. Jackson, J. W. Myerson, F. Stellacci, *Nat. Mater.* **2004**, *3*, 330.
- [36] J. F. Marko, *Macromolecules* **1993**, *26*, 313.
- [37] S. K. Satija, P. D. Gallagher, A. Karim, L. J. Fetters, *Physica B+C (Amsterdam)* **1998**, *248*, 204.
- [38] J. P. Wilcoxon, J. E. Martin, P. Provencio, *J. Chem. Phys.* **2001**, *115*, 998.
- [39] J. P. Wilcoxon, P. Provencio, *J. Phys. Chem. B* **1999**, *103*, 9809.

Mechanically Strong Hydrogels with Ultra-Low Frictional Coefficients

By Daisaku Kaneko, Tomohiro Tada, Takayuki Kurokawa, Jian P. Gong,* and Yoshihito Osada

Industrial or environmental problems caused by materials with high-friction surfaces have always existed. Searching for materials with low-friction surfaces has been a classic and everlasting research topic for materials scientists and engineers. Despite many efforts, it has been shown that surface modification or addition of lubricants is not very effective in reducing the steady-state sliding friction between two solids, which can exhibit a frictional coefficient, μ , of $\sim 10^{-1}$, even in the presence of a lubricant.^[1] One of the most brilliant inventions used to obtain low friction is the bearing system, which exhibits a frictional coefficient much lower than that of sliding friction. The bearing system achieves low friction by using a layer of oil between a surface and a rolling sphere. However,

* Prof. J. P. Gong, D. Kaneko, T. Tada, T. Kurokawa, Prof. Y. Osada
Division of Biological Sciences
Graduate School of Science
Hokkaido University
Sapporo 060-0810 (Japan)
E-mail: gong@sci.hokudai.ac.jp
Prof. J. P. Gong
SORST, JST
Sapporo 060-0810 (Japan)